

Asymmetric Dual-Mode Constellation and Protograph LDPC Code Design for Generalized Spatial MPPM Systems

Liang Lv, Yi Fang, *Member, IEEE*, Lin Dai, Yonghui Li, *Fellow, IEEE*, and
Mohsen Guizani, *Fellow, IEEE*

Abstract

To achieve reliable and efficient transmissions in free-space optical (FSO) communication, this paper designs a new protograph low-density parity-check (PLDPC) coded generalized spatial multipulse position modulation (GSMPPM) system over weak turbulence channels. Specifically, we investigate the PLDPC code, generalized space shift keying (GSSK) modulation, and MPPM constellation. First, we propose a type of novel GSMPPM constellations that intelligently integrate the GSSK into MPPM, referred to as *asymmetric dual-mode (ADM) constellations*, so as to improve the performance of the PLDPC-coded GSMPPM system. Furthermore, exploiting a protograph extrinsic information transfer (PEXIT) algorithm, we construct a type of improved PLDPC code, referred as *IM-PLDPC code*, which outperforms the existing PLDPC codes over weak turbulence channels. Analytical and simulation results show that the proposed ADM constellations and the proposed IM-PLDPC code can obtain noticeable performance gains over their counterparts. Therefore, the proposed PLDPC-coded GSMPPM system with ADM constellations is competent to satisfy the high-reliability requirement for FSO applications.

Index terms— Generalized space shift keying, multipulse pulse-position modulation, protograph low-density parity-check codes, weak turbulence channel, free-space optical communication.

I. INTRODUCTION

Free-space optical (FSO) communication has been widely used for ground-to-satellite communication systems due to high transmission rate and high reliability [1]–[3]. In practical

Liang Lv, Yi Fang, and Lin Dai are with the School of Information Engineering, Guangdong University of Technology, Guangzhou 510006, China (e-mail: lianglv0206@163.com; fangyi@gdut.edu.cn; bs0109dl@163.com).

Yonghui Li is with the School of Electrical and Information Engineering, The University of Sydney, Sydney, NSW 2006, Australia (e-mail: yonghui.li@sydney.edu.au).

Mohsen Guizani is with the Department of Machine Learning, Mohamed Bin Zayed University of Artificial Intelligence (MBZUAI), Abu Dhabi, UAE (e-mail: mguizani@ieee.org).

applications, due to the effect of air refractive index [4], [5], atmospheric turbulence (also known as scintillation) is generated in FSO communication. The atmospheric turbulence causes random fluctuations of the amplitude and phase for the received signal at the receiver, which seriously deteriorate the system performance [6], [7]. To quantify the effect of atmospheric turbulence, several mathematical models have been proposed to describe the distribution of turbulence fading in FSO communication systems. For example, the lognormal distribution has been used to describe weak turbulence channel in FSO communication systems [8], [9].

The weak turbulence channel is one of the most typical channel models to describe FSO communication scenarios, which have attracted significant research interest in the past two decades [10], [11]. In the FSO communication systems based on weak turbulence, the optical signal uses intensity modulation with direct detection (IM/DD) [12], which mainly adopts pulse position modulation (PPM) [13] or on-off keying modulation (OOK) [14]. Although OOK can provide high bandwidth efficiency, it suffers low energy efficiency and high synchronization complexity at the receiver [15]. As an alternative, PPM can improve the energy efficiency by increasing the order of modulation [13]. However, the improvement of energy efficiency is obtained at cost of bandwidth efficiency, which leads limited transmission capacity. As a variant of PPM, multipulse position modulation (MPPM) has been proposed to improve the bandwidth efficiency by utilizing multiple pulsed slots during each symbol transmission [16]. In the past decade, researchers have conceived various designs of MPPM constellations in FSO communication systems. In [4], a Gray labeling search (GLS) algorithm which considers the Hamming distance between adjacent symbols has been proposed to construct a new type of MPPM constellations. Furthermore, the authors in [17] have proposed a new subset selection (MCSS) algorithm to construct MPPM constellations. The above two MPPM constellations have been only employed in single-input-single-output (SISO) technique, which cannot attain spatial diversity.

To tackle the above issue, multiple-input multiple-output (MIMO) technique has been introduced in FSO communication systems [18]. To be specific, in [19], a low-complexity spatial pulse position modulation (SPPM) scheme that combines SSK with PPM has been proposed. Furthermore, the authors in [20] have developed a generalized SPPM (GSPPM) scheme by using multiple transmit antennas to send the same PPM symbols at each transmission instant. In addition, a spatial MPPM (SMPPM) scheme adopting SSK and MPPM has been considered in [21]. So far, an in-depth investigation on GSMPPM is still lacking. Actually, a GSMPPM

constellation includes a spatial-domain constellation (i.e., effective activated antenna groups) and a signal-domain constellation (i.e., MPPM constellations). The sizes of both two types of constellations are a power of two, and thus part of antenna groups and MPPM symbols keep idle. Therefore, how to design an efficient GSMPPM constellation using more antenna groups and MPPM symbols is a challenging problem.

An alternative method to improve the system performance is the employment of error-correction codes (ECCs). For example, Reed-solomon (RS) codes [15], [22] and Low-density parity-check (LDPC) codes [23], [24] have been used in the FSO systems. Among all ECCs, a class of structured LDPC codes, i.e., protograph LDPC (PLDPC) codes [25], have received tremendous attention due to low complexity and close-to-capacity performance [26]. As well, the researchers have proposed a protograph extrinsic information transfer (PEXIT) [27] algorithm for predicting the decoding thresholds of PLDPC codes in specific communication scenarios. With the aid of PEXIT algorithm, the authors have constructed a PLDPC code (i.e., code-B) for Poisson channels [28]. Nevertheless, the code-B PLDPC code may not perform well over weak turbulence channels due to the different distribution characteristics. Hence, it is crucial to design a type of PLDPC code tailored for the PLDPC-coded GSMPPM system over such a scenario.

Inspired by the above motivation, we make a comprehensive investigation on the PLDPC-coded GSMPPM systems over weak turbulence channels. Thus, the contributions of this work are summarized as follows.

1. We propose a new GSMPPM scheme based on an asymmetric dual-mode (ADM) constellation search algorithm by removing the constraint condition that the sizes of spatial-domain constellation and signal-domain constellation must be a power of two.
2. We analyze the constellation-constrained capacity of the proposed GSMPPM constellations in the case of using different MPPM slots.
3. With the aid of PEXIT algorithm, we construct an improved PLDPC code (i.e., IM-PLDPC code) to achieve excellent decoding thresholds in the GSMPPM system.
4. Analytical and simulation results reveal that the proposed PLDPC-coded ADM-aided GSMPPM system remarkably outperforms the existing counterparts over weak turbulence channels.

The remainder of this paper is organized as follows. In Section II, we propose the PLDPC-coded GSMPPM system and estimate its corresponding constellation-constrained capacity. In Section III, we present the design method of the ADM constellations. In Section IV, we construct a new PLDPC code for the PLDPC-coded GSMPPM system. Simulation results are presented

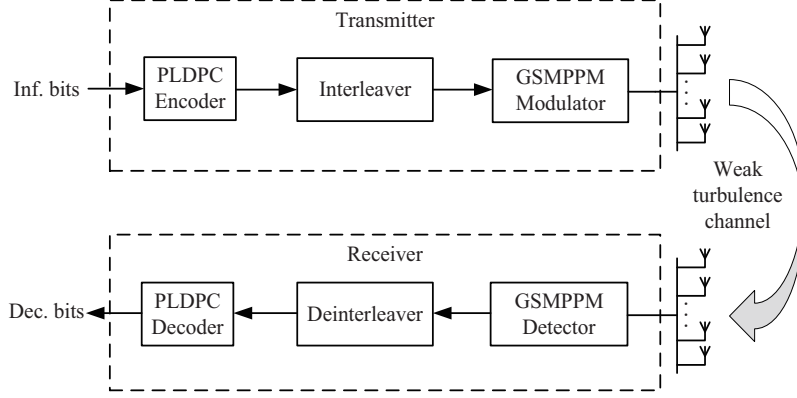


Fig. 1. Block diagram of a PLDPC-coded GSMPPM system over a weak turbulence channel.

in Section V, and the conclusion is made in Section VI.

II. SYSTEMS MODEL

A. PLDPC-Coded GSMPPM System

The block diagram of a PLDPC-coded GSMPPM system is shown in Fig. 1, which has N_t transmit antennas and N_r receive antennas. At each transmission instant, N_a ($2 \leq N_a \leq N_t$) out of N_t transmit antennas are chosen as an activated antenna group to transmit signals in the PLDPC-coded GSMPPM systems. In the conventional GSMPPM system, $2^{\lfloor \log_2^{N_s} \rfloor}$ effective activated antenna groups are selected to transmit symbols, and each activated antenna group is used to transmit an MPPM symbol, where $N_s = \binom{N_t}{N_a}$ is the number of all possible activated antenna groups, $\binom{a}{b}$ denotes the combinatorial number operator and $\lfloor \cdot \rfloor$ denotes the floor function. Specifically, at the transmitter, a length- k information-bit sequence $\mathbf{u} = \{u_1, u_2, \dots, u_k\}$ is first encoded by a PLDPC encoder to generate a length- s codeword $\mathbf{c} = \{c_1, c_2, \dots, c_s\}$. Subsequently, \mathbf{c} is passed to a GSMPPM modulator after permuted by a random interleaver. After that, every m coded bits are divided into two parts, the first $m_t = \lfloor \log_2^{N_s} \rfloor$ coded bits are used to select the effective activated antenna group, while the remaining $m_s = \log_2^M$ coded bits are mapped into an M -ary MPPM symbol. Thus, a length- (s/m) GSMPPM symbol sequence $\mathbf{Z} = \{\mathbf{z}_1, \mathbf{z}_2, \dots, \mathbf{z}_{s/m}\}$ can be yielded. Generally, each MPPM symbol consists of l slots, with l_a ($2 \leq l_a < l/2$) pulsed slots and $(l - l_a)$ non-pulsed slots. Thereby, the MPPM symbol can be characterized by a length- l vector $\mathbf{z}_p = [z_p^1, z_p^2, \dots, z_p^l]$, where $z_p^q \in \{0, 1\}$, $q = 1, 2, \dots, l$, $p = 1, 2, \dots, s/m$. In the vector \mathbf{z}_p , “1” represents a pulsed slot and “0” means a non-pulsed slot. Note that we use

$(N_t, N_r, N_a, l, l_a, M_s)$ to represent a GSMPPM constellation with size of $M_s = 2^m$ in this paper. Finally, the GSMPPM symbol sequence \mathbf{Z} is passed through a weak turbulence channel and each GSMPPM symbol z_p is converted into a transmission vector \mathbf{x} . The channel output \mathbf{y} can be written as

$$\mathbf{y} = \frac{P_t}{\sqrt{N_a}} \mathbf{H} \mathbf{x} + \mathbf{w}, \quad (1)$$

where $\mathbf{y} = [\mathbf{y}_1, \mathbf{y}_2, \dots, \mathbf{y}_{N_r}]^T$ denotes the received signal vector with size of $N_r \times 1$ by all receive antennas, $\mathbf{y}_i = [y_i^1, y_i^2, \dots, y_i^l]$ is the received signal in the i th receive antenna; $\mathbf{x} = [\mathbf{x}_1, \mathbf{x}_2, \dots, \mathbf{x}_{N_t}]^T$ denotes the GSMPPM signal vector with size of $N_t \times 1$ sent by transmit antennas, $\mathbf{x}_j = [x_j^1, x_j^2, \dots, x_j^l]$ is the GSMPPM signal sent by the j th transmit antenna; \mathbf{w} denotes the noise matrix with size of $N_r \times l$, in which each element is the real additive Gaussian noise with zero-mean and variance $\sigma^2 = N_0/2$, N_0 is the noise power spectral density. Moreover, $P_t = P_a \cdot \gamma$ denotes the peak transmit power, where P_a is the average transmit power (all modulation patterns use the same P_a), $\gamma = 1/\tau$ is the peak-to-average power ratio (PAPR), and $\tau = l_a/l$ is the duty cycle of each MPPM symbol. In addition, $\mathbf{H} = (h_{ij})$ denotes the channel gain matrix of size $N_r \times N_t$, where h_{ij} is the channel coefficient from the j th transmit antenna to the i th receive antenna in the PLDPC-coded GSMPPM system. The channel coefficient h_{ij} follows a lognormal distribution, and its probability density function (PDF) is given by [8]

$$f(h_{ij}) = \frac{1}{2h_{ij}\sqrt{2\pi}\sigma_x} \exp\left(-\frac{(\ln(h_{ij}) - 2\mu)^2}{8\sigma_x^2}\right), \quad (2)$$

where $\sigma_x^2 = 0.25 \ln(1 + \sigma_I^2)$ and σ_I ($\sigma_I^2 < 1$) is the channel scintillation index [29]. To ensure that the average power is not impacted by channel fading, the channel coefficients are normalized as $\mathbb{E}[h_{ij}^2] = 1$, where $\mathbb{E}[\cdot]$ stands for the expectation function. The signal-to-noise ratio (SNR) can be expressed as [19], [20] $\text{SNR} = (l_a P_t^2) / (2Rm\sigma^2)$, where R is the code rate.

At the receiver, the received signal \mathbf{y} is detected by the max-sum approximation of log-domain maximum a-posterior probability (Max-log-MAP) algorithm [15], [30] in the GSMPPM detector. Then, the extrinsic log-likelihood ratios (LLRs) output from the GSMPPM detector are sent to a deinterleaver. After that, these extrinsic LLRs will be fed to a PLDPC decoder to perform belief-propagation (BP) [31], [32] decoding.

B. Constellation-Constrained Capacity

Given the channel state information (CSI), the maximum rate of a reliable transmission can be determined by the average mutual information (AMI) [33]. Assume that the selected GSMPPM

symbol from the GSMPPM constellation is equiprobable, the constellation-constrained AMI of a code modulation (CM) scheme over a weak turbulence channel can be calculated as [34]

$$C_{\text{CM}} = m - \mathbb{E}_{\mathbf{x}, \mathbf{y}, \mathbf{H}} \left[\log_2 \frac{\sum_{\mathbf{r} \in \Omega} p(\mathbf{y} | \mathbf{r}, \mathbf{H})}{p(\mathbf{y} | \mathbf{x}, \mathbf{H})} \right], \quad (3)$$

where

$$\begin{aligned} p(\mathbf{y} | \mathbf{x}, \mathbf{H}) &= \prod_{i=1}^{N_r} \prod_{q=1}^l p(y_i^q | \mathbf{x}, \mathbf{H}) \\ &= \frac{\exp \left[-\frac{\sum_{i=1}^{N_r} \sum_{q=1}^l \left(y_i^q - \sum_{j=1}^{N_t} \frac{P_t}{\sqrt{N_a}} h_{ij} x_j^q \right)^2}{2\sigma^2} \right]}{i^{N_r} \sqrt{2\pi\sigma^2}}. \end{aligned} \quad (4)$$

In Eq. (3), Ω denotes a GSMPPM constellation, y_i^q denotes the received signal of the q th slot at the i th receive antenna, x_j^q denotes the signal transmitted by the q th slot at the j th transmit antenna, and $p(\mathbf{y} | \mathbf{x}, \mathbf{H})$ is the conditional probability density function (PDF) of the channel output \mathbf{y} . In addition, the constellation-constrained AMI of a bit-interleaved coded modulation (BICM) scheme can be calculated as [34]

$$C_{\text{BICM}} = m - \sum_{k=1}^m \mathbb{E}_{b, \mathbf{y}, \mathbf{H}} \left[\log_2 \frac{\sum_{\mathbf{x} \in \Omega} p(\mathbf{y} | \mathbf{x}, \mathbf{H})}{\sum_{\mathbf{x} \in \Omega_k^b} p(\mathbf{y} | \mathbf{x}, \mathbf{H})} \right], \quad (5)$$

where Ω_k^b denotes the subset of GSMPPM constellation Ω with the k th bit being $b \in \{0, 1\}$.

III. DESIGN OF PROPOSED ADM CONSTELLATIONS FOR PLDPC-CODED GSMPPM SYSTEM

A. Proposed ADM Constellations

In the conventional GSMPPM modulation scheme, the m_t coded bits are used to select effective activated antenna groups, while the m_s coded bits are modulated by using MPPM symbols for effective activated antenna groups. Note that each effective activated antenna group shares the same MPPM constellation set $\Psi = \{\Psi_1, \Psi_2, \dots, \Psi_M\}$. In practice, the signal-domain constellation set Φ consists of full MPPM symbols with size of $M_{\max} = \binom{l}{l_a}$, while the spatial-domain constellation includes N_s possible activated antenna groups. As seen, the sizes of both constellations are typically not a power of two. For this reason, Φ cannot be directly used for bit-to-symbol mapping in the proposed system and certain activated antenna groups cannot be exploited substantially. For instance, when $N_t = 4$ and $N_a = 2$, (1, 2), (3, 4), (1, 4) and (2, 3) are selected as effective activated antenna groups, while the remaining activated antenna groups

Algorithm 1: ADM Constellation Parameter Selection

- 1 **Initialization:** Given parameters N_t , N_a , l and l_a , calculate N_s , M_{\max} , M_s and $M \leftarrow 2^{\lfloor \log_2 M_{\max} \rfloor}$. Set $Th = 0$, $i = 0$, $N_{\text{add}} \leftarrow N_s - 2^{m_t}$.
 - 2 **while** $Th == 0$ **do**
 - 3 Calculate $M_A \leftarrow \lceil M_s/N_s \rceil + i$ and M_B ;
 - 4 **if** $(M_A > M_B)$ && $(M_A + M_B) \leq M_{\max}$ **then**
 - 5 $Th = 1$;
 - 6 **continue**
 - 7 $N_{\text{add}} \leftarrow N_{\text{add}} - 1$;
 - 8 **if** $N_{\text{add}} == 0$ **then**
 - 9 Reset N_{add} and $i \leftarrow i + 1$;
 - 10 **Finalization:** Output parameters: N_{add} , M_{\max} , M , m , M_A and M_B .
-

(1, 3) and (2, 4) are idle, where 1, 2, 3 and 4 denote the corresponding transmit antenna index. Meanwhile, in the existing works, e.g., GLS [4] and MCSS [17] constellations, only M MPPM symbols are selected from set Φ as an eligible sub-constellation set $\Psi \subset \Phi$ to perform the bit-to-symbol mapping. To overcome the above weakness, we proposed a type of asymmetric dual-mode (ADM) constellations by considering full-MPPM symbols and all possible activated antenna groups as much as possible. The detailed design steps of the proposed ADM constellations in the PLDPC-coded GSMPPM system are as follows.

- 1) **ADM Constellation Parameter Selection:** In order to utilize all activated antenna groups as much as possible, how to determine the number N_{add} of additional activated antenna groups is one of the most critical issues. Given system parameters N_t , N_a , l , l_a and M_s , all possible activated antenna groups can be calculated as N_s and the number of full-MPPM symbols is M_{\max} . First, we randomly select 2^{m_t} as effective activated antenna groups, thus the number of the remaining activated antenna groups is $N_s - 2^{m_t}$. The additional activated antenna groups are selected from the remaining activated antenna groups. We define two MPPM constellation sets Ψ_A and Ψ_B . As such, each effective activated antenna group sends GSMPPM symbols by using constellation set Ψ_A with size of M_A , while each additional activated antenna group sends GSMPPM symbols by using constellation set Ψ_B with size of

M_B . Finally, the relationship between the M_A , M_B , and N_{add} can be represented as

$$\begin{aligned} M_B &= \lceil (M_s - 2^{m_t} \cdot M_A) / N_{\text{add}} \rceil, \\ \text{subject to : } M_A &> M_B, \\ M_A + M_B &\leq M_{\text{max}}, \end{aligned} \quad (6)$$

where the initial value of M_A is set to $\lceil M_s / N_s \rceil$ and the initial value of N_{add} is set to $N_s - 2^{m_t}$. To elaborate further, the ADM constellation parameter selection is summarized in *Algorithm 1*.

- 2) **ADM Constellation Formulation:** (i) The parameters N_{add} , M_A and M_B of an ADM constellation are determined by *Algorithm 1*. Considering an ADM GSMPPM constellation scheme with M_s MPPM symbols, there exist M_s labels in the corresponding constellations mapper, each label $\xi_\alpha = [\xi_\alpha^1, \xi_\alpha^2, \dots, \xi_\alpha^m]$ consists of m labeling bits, where $\alpha = 1, 2, \dots, M_s$, $\xi_\alpha^m \in \{0, 1\}$, and ξ_α is the binary representation of the index value $(\alpha - 1)$. To conveniently determine the MPPM symbols in sub-constellation set Ψ_A , we first divide the $2^{m_t} M_A$ labels into 2^{m_t} label subsets. The index values corresponding to the labels in the λ th label subset ξ_λ within Ψ_A belong to the interval $[\lambda M, (\lambda + 1)M]$ (see Table I), and the remaining labels correspond to the MPPM symbols in sub-constellation set Ψ_B , where $\lambda = 0, 1, \dots, 2^{m_t} - 1$. Here, we take the λ th label subset ξ_λ as an example and select the corresponding sub-constellation set Ψ_A . Especially, M_A MPPM symbols must be selected from a full-MPPM symbols constellation set Φ of size M_{max} to constitute an MPPM sub-constellation set Ψ_{A_p} , where $p = 1, 2, \dots, \binom{M_{\text{max}}}{M_A}$. The i th MPPM sub-constellation symbol (i.e., $\Psi_{A_p, i} = [\psi_{A_p, i}^1, \psi_{A_p, i}^2, \dots, \psi_{A_p, i}^l]$) can be marked by the i th label (i.e., $\xi_{\lambda, i} = [\xi_{\lambda, i}^1, \xi_{\lambda, i}^2, \dots, \xi_{\lambda, i}^m]$) in ξ_λ , where $i = 1, 2, \dots, M_A$. Further, the Hamming distance of arbitrary two different MPPM symbols (e.g., $\Psi_{A_p, i}$ and $\Psi_{A_p, j}$) is defined as D^{ij} . One can calculate the Hamming distance $D_{A_p, i} = \frac{1}{M_A - 1} \sum_{j=1, i \neq j}^{M_A} D^{ij}$ between the i th MPPM symbol $\Psi_{A_p, i}$ and the remaining $M_A - 1$ MPPM symbols. Then, the average Hamming distance of the sub-constellation Ψ_{A_p} can be obtained by $D_{a, p} = \frac{1}{M_A} \sum_{i=1}^{M_A} D_{A_p, i}$. Assume that $D_{a, p}$ is the maximum average Hamming distance D_a , we select the sub-constellation Ψ_{A_p} for the next operation. For the sub-constellation set Ψ_{A_p} , we relabel each MPPM symbol based on the maximum Hamming distance criterion. To be specific, when $D^{ij} = 2l_a$ (i.e., the largest Hamming distance), we maximize the Hamming distance d of arbitrary two different labels corresponding to two different MPPM symbols

Algorithm 2: ADM Constellation Formulation

```

1 Initialization: Given parameters  $N_{\text{add}}, M_A, M_B, M_{\text{max}}, M, m, l$  and  $l_a$ , generate a
   full-MPPM symbols set  $\Phi$  of size  $M_{\text{max}}$ . Set  $D_a = 0, D_b = 0, \text{Label} = 0$ .
2 for  $p = 1, 2, \dots, \binom{M_{\text{max}}}{M_A}$  do
3   Generate a sub-constellation  $\Psi_{A,p}$  and calculate  $D_{a,p}$ ;
4   if  $D_{a,p} > D_a$  then
5     Label  $\leftarrow p; D_a \leftarrow D_{a,p}$ ;
6 for  $i = 1, 2, \dots, M_A$  do
7   for  $j = i + 1, i + 2, \dots, M_A$  do
8     if  $D^{ij} == 2l_a$  then
9       Maximize the Hamming distance  $d$  between two different labels in  $\xi_\lambda$ ;
10  $\Psi_A \leftarrow \Psi_{A,\text{Label}}$ .
11 Remove MPPM symbols in  $\Psi_A$  from  $\Phi$ , i.e.,  $\Phi = \Phi/\Psi_A$ .
12 for  $\eta = 1, 2, \dots, \binom{M_{\text{max}} - M_A}{M_B}$  do
13   Generate a sub-constellation  $\Psi_{B,\eta}$  and calculate  $D_{b,\eta}$ ;
14   if  $D_{b,\eta} > D_b$  then
15     Label  $\leftarrow \eta; D_b \leftarrow D_{b,\eta}$ ;
16 for  $i = 1, 2, \dots, M_B$  do
17   for  $j = i + 1, i + 2, \dots, M_B$  do
18     if  $D^{ij} == 2l_a$  then
19       Maximize the Hamming distance  $d$  between two different labels in  $\zeta_\mu$ ;
20  $\Psi_B \leftarrow \Psi_{B,\text{Label}}$ .
21 Finalization: Output  $\Psi_A, \Psi_B$ .

```

$\Psi_{A,p,i}$ and $\Psi_{A,p,j}$. If the case of $d = m$ does not exist, we consider $d = m - 1, m - 2, \dots, 1$ and so on. Based on the above operations, we can obtain a sub-constellation set Ψ_A .

(ii) In order to decrease the interference between GSMPPM symbols in two different activated antenna groups, the same MPPM symbol cannot exist in both Ψ_A and Ψ_B . Thus, we should

remove all MPPM symbols belonging to Ψ_A from Φ (i.e., $\bar{\Phi}_A = \Phi/\Psi_A$). Given a spectral efficiency ρ , the additional activated antenna groups will cause the truncation of the effective activated antenna groups corresponding to signal-domain constellations. For example, when $N_t = 4$, $N_a = 2$, and $M_A = 6$, two MPPM symbols corresponding to the labels [00110] and [00111] cannot combine with the effective activated antenna groups to form two GSMPPM symbols, it can only form two GSMPPM symbols with the additional activated antenna groups (1, 3) and (2, 4), respectively. Therefore, we reclassify the remaining M_r labels into N_{add} label subsets in a sequential order, where $M_r = 2^m(M - M_A)$. When $M - M_A \leq N_{\text{add}}$, the index value corresponding to the β th label in the μ th label subset ζ_μ is $(\beta-1)M + M_A + \mu$, where $\mu = 0, 1, \dots, N_{\text{add}}-1$, $\beta = 1, 2, \dots, M_B$ (see Table I). Otherwise (i.e., $M - M_A > N_{\text{add}}$), the index values corresponding to the labels are divided evenly into N_{add} subsets in a sequential order (see Table II). Especially, each label in a label subset ζ_μ corresponds to an MPPM symbol in sub-constellation Ψ_B^1 . Taking the label subset ζ_μ as an example, we select M_B MPPM symbols from set $\bar{\Phi}_A$ to form a sub-constellation $\Psi_{B,\eta}$, where $\eta = 1, 2, \dots, \binom{M_{\text{max}} - M_A}{M_B}$. Likewise, we calculate the average Hamming distance of the sub-constellation $\Psi_{B,\eta}$, which can be obtain by $D_{b,\eta} = \frac{1}{M_B(M_B-1)} \sum_{i=1}^{M_B} \sum_{j=1, i \neq j}^{M_B} D^{ij}$. Assume that $D_{b,\eta}$ is the maximum average Hamming distance D_b , we select the sub-constellation $\Psi_{B,\eta}$ for the next operation. Then, when $D^{ij} = 2l_a$ (i.e., the largest Hamming distance), we maximize the Hamming distance d of arbitrary two different labels corresponding to two MPPM symbols $\Psi_{B,\eta,i}$ and $\Psi_{B,\eta,j}$. Finally, the subconstellation set Ψ_B can be obtained by the above operation.

Based on the above two steps, a type of ADM constellations can be formulated. To illustrate further, the design method for ADM constellations is summarized in *Algorithm 2*. For example, with the aid of *Algorithm 2*, the ADM constellations with spectral efficiencies $\rho = 5$ bits per channel use (bpcu) and $\rho = 6$ bpcu are shown in Tables I and II, respectively.

B. Performance Analysis

To verify the effectiveness of the proposed ADM constellations, the CM and BICM capacities of different GSMPPM constellations can be calculated by using the constellation-constrained capacity analysis method in Section II-B. In the PLDPC-coded GSMPPM systems, we calculate the constellation-constrained capacities of the proposed ADM constellations, the optimized

¹The selected sub-constellation sets Ψ_A and Ψ_B are also applicable to other label subsets ξ_λ and ζ_μ , respectively.

TABLE I

MAPPING RELATIONSHIP AMONG LABELS, MPPM SYMBOLS AND ACTIVATED ANTENNA GROUPS FOR THE PROPOSED ADM CONSTELLATIONS, WHERE $N_t = 4$, $N_r = 4$, $N_t = 2$, AND $\rho = 5$ BPCU (I.E., $l = 5$, $l_a = 2$ AND $l = 6$, $l_a = 2$).

Effective activated antenna group	Index value	Label ξ	Ψ_A ($l = 5$)	Ψ_A ($l = 6$)	Effective activated antenna group	Index value	Label ξ	Ψ_A ($l = 5$)	Ψ_A ($l = 6$)
(1, 2)	0	0 0 0 0 0	1 0 1 0 0	1 1 0 0 0 0	(3, 4)	8	0 1 0 0 0	1 0 1 0 0	1 1 0 0 0 0
	1	0 0 0 0 1	0 1 1 0 0	0 0 1 0 0 1		9	0 1 0 0 1	0 1 1 0 0	0 0 1 0 0 1
	2	0 0 0 1 0	1 0 0 1 0	0 1 0 1 0 0		10	0 1 0 1 0	1 0 0 1 0	0 1 0 1 0 0
	3	0 0 0 1 1	0 0 1 1 0	0 0 1 1 0 0		11	0 1 0 1 1	0 0 1 1 0	0 0 1 1 0 0
	4	0 0 1 0 0	1 0 0 0 1	1 0 0 0 1 0		12	0 1 1 0 0	1 0 0 0 1	1 0 0 0 1 0
	5	0 0 1 0 1	0 1 0 0 1	0 0 0 0 1 1		13	0 1 1 0 1	0 1 0 0 1	0 0 0 0 1 1
(1, 4)	16	1 0 0 0 0	1 0 1 0 0	1 1 0 0 0 0	(2, 3)	24	1 1 0 0 0	1 0 1 0 0	1 1 0 0 0 0
	17	1 0 0 0 1	0 1 1 0 0	0 0 1 0 0 1		25	1 1 0 0 1	0 1 1 0 0	0 0 1 0 0 1
	18	1 0 0 1 0	1 0 0 1 0	0 1 0 1 0 0		26	1 1 0 1 0	1 0 0 1 0	0 1 0 1 0 0
	19	1 0 0 1 1	0 0 1 1 0	0 0 1 1 0 0		27	1 1 0 1 1	0 0 1 1 0	0 0 1 1 0 0
	20	1 0 1 0 0	1 0 0 0 1	1 0 0 0 1 0		28	1 1 1 0 0	1 0 0 0 1	1 0 0 0 1 0
	21	1 0 1 0 1	0 1 0 0 1	0 0 0 0 1 1		29	1 1 1 0 1	0 1 0 0 1	0 0 0 0 1 1
Additional activated antenna group	Index value	Label ζ	Ψ_B ($l = 5$)	Ψ_B ($l = 6$)	Additional activated antenna group	Index value	Label ζ	Ψ_B ($l = 5$)	Ψ_B ($l = 6$)
(1, 3)	6	0 0 1 1 0	1 1 0 0 0	0 1 0 0 0 1	(2, 4)	7	0 0 1 1 1	1 1 0 0 0	0 1 0 0 0 1
	14	0 1 1 1 0	0 1 0 1 0	0 0 1 0 1 0		15	0 1 1 1 1	0 1 0 1 0	0 0 1 0 1 0
	22	1 0 1 1 0	0 0 1 0 1	0 0 0 1 0 1		23	1 0 1 1 1	0 0 1 0 1	0 0 0 1 0 1
	30	1 1 1 1 0	0 0 0 1 1	0 0 0 1 1 0		31	1 1 1 1 1	0 0 0 1 1	0 0 0 1 1 0

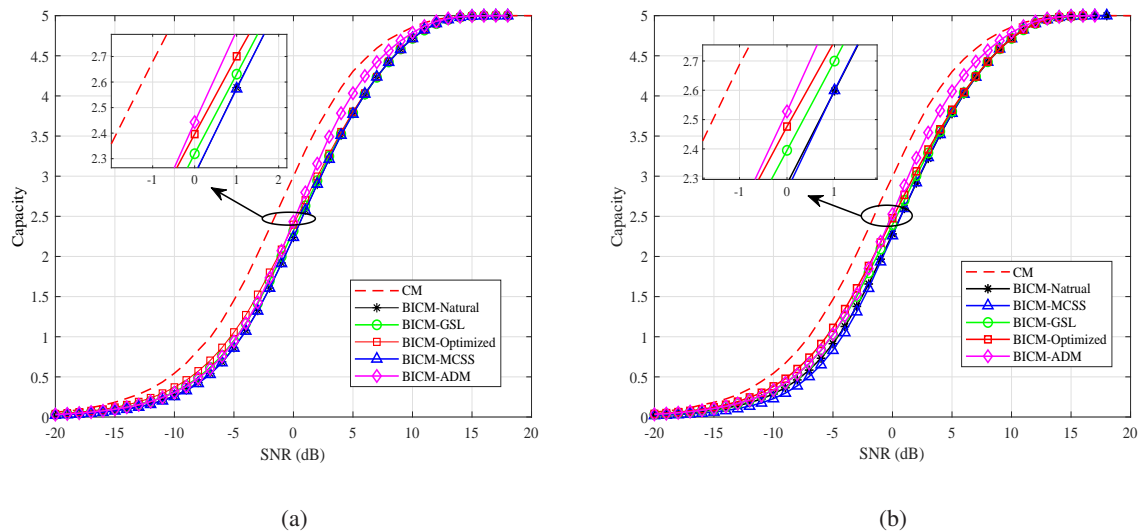


Fig. 2. Capacities of the PLDPC-coded GSMPPM systems with the proposed ADM constellation, the optimized constellation, natural constellation, MCSS constellation, and GLS constellation: (a) $(4, 4, 2, 5, 2, 32)$ -GSMPPM with $\rho = 5$ bpcu; (b) $(4, 4, 2, 6, 2, 32)$ -GSMPPM with $\rho = 5$ bpcu.

constellations², natural constellation [35], MCSS constellation [17], and GLS constellation [4] with $\rho = 5$ bpcu and $\rho = 6$ bpcu are illustrated in Fig. 2 and Fig. 3, respectively, where

²The optimized constellations are special cases of the proposed ADM constellations, which can be obtained by *Algorithm 2* with the assumption of $N_{\text{add}} = 0$, $M_A = M$ and $M_B = 0$.

TABLE II

MAPPING RELATIONSHIP AMONG LABELS, MPPM SYMBOLS AND ACTIVATED ANTENNA GROUPS FOR THE PROPOSED ADM CONSTELLATIONS, WHERE $N_t = 4$, $N_r = 4$, $N_a = 2$, AND $\rho = 6$ BPCU (I.E., $l = 7$, $l_a = 2$ AND $l = 8$, $l_a = 2$).

Effective activated antenna group	Index value	Label ξ	Ψ_A ($l = 7$)	Ψ_A ($l = 8$)	Effective activated antenna group	Index value	Label ξ	Ψ_A ($l = 7$)	Ψ_A ($l = 8$)	
(1, 2)	0	000000	0000011	00100100	(3, 4)	16	010000	0000011	00100100	
	1	000001	0010001	00110000		17	010001	0010001	00110000	
	2	000010	0001010	00001010		18	010010	0001010	00001010	
	3	000011	1001000	00010010		19	010011	1001000	00010010	
	4	000100	0100010	10000100		20	010100	0100010	10000100	
	5	000101	0110000	10010000		21	010101	0110000	10010000	
	6	000110	1000010	00001100		22	010110	1000010	00001100	
	7	000111	1100000	10001000		23	010111	1100000	10001000	
	8	001000	0000101	01000001		24	011000	0000101	01000001	
	9	001001	0010100	00100001		25	011001	0010100	00100001	
	10	001010	0001100	01000010	26	011010	0001100	01000010		
(1, 4)	32	100000	0000011	00100100	(2, 3)	48	110000	0000011	00100100	
	33	100001	0010001	00110000		49	110001	0010001	00110000	
	34	100010	0001010	00001010		50	110010	0001010	00001010	
	35	100011	1001000	00010010		51	110011	1001000	00010010	
	36	100100	0100010	10000100		52	110100	0100010	10000100	
	37	100101	0110000	10010000		53	110101	0110000	10010000	
	38	100110	1000010	00001100		54	110110	1000010	00001100	
	39	100111	1100000	10001000		55	110111	1100000	10001000	
	40	101000	0000101	01000001		56	111000	0000101	01000001	
	41	101001	0010100	00100001		57	111001	0010100	00100001	
		42	101010	0001100		01000010	58	111010	0001100	01000010
	Additional activated antenna group	Index value	Label ζ	Ψ_B ($l = 7$)		Ψ_B ($l = 8$)	Additional activated antenna group	Index value	Label ζ	Ψ_B ($l = 7$)
(1, 3)	11	001011	0010010	10100000	(2, 4)	43	101011	0010010	10100000	
	12	001100	0001001	01010000		44	101100	0001001	01010000	
	13	001101	0011000	01001000		45	101101	0011000	01001000	
	14	001110	1000001	01100000		46	101110	1000001	01100000	
	15	001111	1010000	00101000		47	101111	1010000	00101000	
	27	011011	0000110	10000010		59	111011	0000110	10000010	
	28	011100	0100001	00010100		60	111100	0100001	00010100	
	29	011101	0101000	00010001		61	111101	0101000	00010001	
	30	011110	0100100	00000101		62	111110	0100100	00000101	
		31	011111	1000100		00000011	63	111111	1000100	00000011

$N_t = 4$, $N_r = 4$, $N_a = 2$ and $\sigma_x = 0.3$. For the case of (4, 4, 2, 5, 2, 32) GSMPPM scheme with $\rho = 5$ bpcu, in Fig. 2(a), one can see that the proposed ADM constellation and the optimized constellation can obtain much larger capacities than the other three constellations when the code rate $R > 0.35$ (i.e., $R = \mathcal{C}_{\text{BICM}}/m$). In particular, the proposed ADM constellation is closest to the CM capacity. In Fig. 2(b), we can observe similar results for (4, 4, 2, 6, 2, 32) GSMPPM scheme. Likewise, the same phenomenon can be observed when spectral efficiency $\rho = 6$ bpcu (see Fig. 3). Therefore, it can be concluded that the proposed ADM constellations are able to obtain better performance with respect to the existing counterparts in the PLDPC-coded GSMPPM systems.

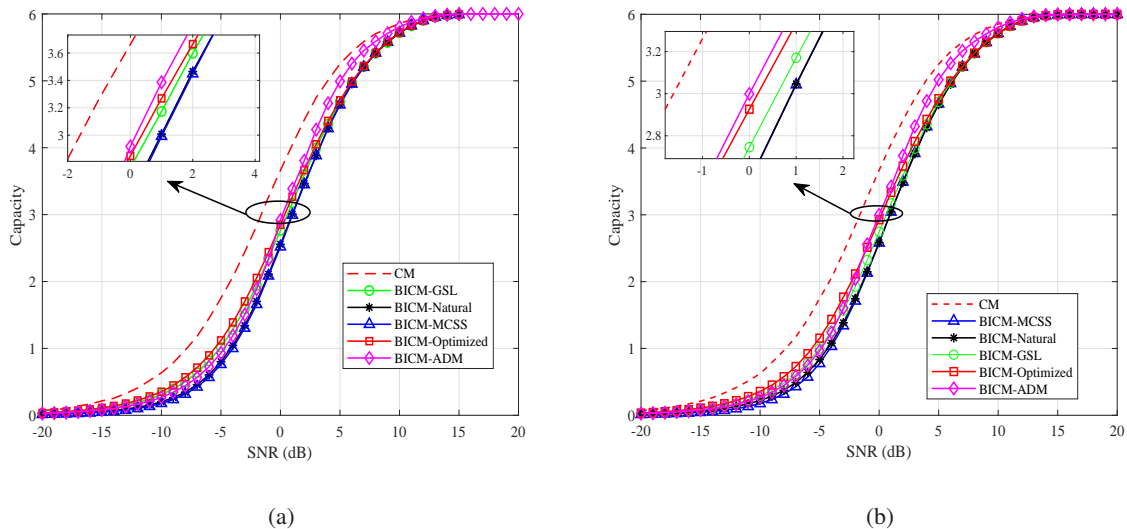


Fig. 3. Capacities of the PLDPC-coded GSMPPM systems with the proposed ADM constellation, the optimized constellation, natural constellation, MCSS constellation, and GLS constellation: (a) $(4, 4, 2, 7, 2, 64)$ -GSMPPM with $\rho = 6$ bpcu; (b) $(4, 4, 2, 8, 2, 64)$ -GSMPPM with $\rho = 6$ bpcu.

To further verify the advantage of our proposed ADM constellations, the decoding thresholds of a code rate- $1/2$ accumulate-repeat-by-4-jagged-accumulate (AR4JA) code [27] in the PLDPC-coded GSMPPM systems are analysed by utilizing the PEXIT algorithm [33], [36]. In addition, the optimized, natural, GSL and MCSS constellations are used as benchmarks. Note that the transmitted codeword length is assumed to be 4500 and the maximum number of BP iterations t_{BP} is set to be 100. As can be seen from Table III, in the cases of $(4, 4, 2, 5, 2, 32)$ and $(4, 4, 2, 6, 2, 32)$ GSMPPM schemes (i.e., $\rho = 5$ bpcu), the decoding thresholds of the AR4JA code with the proposed ADM constellation and the optimized constellation are smaller than those with other three existing constellations. When the spectral efficiency $\rho = 6$ bpcu (i.e., $(4, 4, 2, 7, 2, 64)$ and $(4, 4, 2, 8, 2, 64)$ GSMPPM schemes), the proposed ADM constellations still have excellent error performance. Importantly, the decoding thresholds of the proposed ADM constellations are the lowest, which indicates that our proposed ADM constellations are the best scheme for the PLDPC-coded GSMPPM systems.

IV. DESIGN AND ANALYSIS OF PLDPC CODES FOR ADM-AIDED GSMPPM SYSTEM

A. Proposed IM-PLDPC Code

A PLDPC code is represented by a Tanner graph, which consists of several small sets of check nodes (CNs), variable nodes (VNs), and edges [25], [27]. The VNs and CNs are connected by

TABLE III

DECODING THRESHOLDS (I.E., dB) OF THE AR4JA CODE IN THE GSMPPM SYSTEMS WITH THE PROPOSED ADM CONSTELLATION, THE OPTIMIZED CONSTELLATION, NATURAL CONSTELLATION, MCSS CONSTELLATION, AND GLS CONSTELLATION OVER A WEAK TURBULENCE CHANNEL, WHERE $N_t = 4$, $N_r = 4$, $N_t = 2$, AND THE MODULATION PATTERNS ARE (4, 4, 2, 5, 2, 32), (4, 4, 2, 6, 2, 32), (4, 4, 2, 7, 2, 64) AND (4, 4, 2, 8, 2, 64).

Modulation Pattern \ Constellation	(4, 4, 2, 5, 2, 32)	(4, 4, 2, 6, 2, 32)	(4, 4, 2, 7, 2, 64)	(4, 4, 2, 8, 2, 64)
Natural	-3.0734	-3.1872	-3.6949	-3.7976
MCSS	-2.9364	-3.1692	-3.6861	-3.8987
GLS	-3.2572	-3.3928	-4.0969	-4.1966
Optimized	-3.4875	-3.7466	-4.2324	-4.3361
ADM	-3.6942	-3.8542	-4.3475	-4.4732

TABLE IV

DECODING THRESHOLDS (I.E., dB) OF THE AR4JA CODE, REGULAR-(3,6) CODE, THE OPTIMIZED CODE-B AND THE PROPOSED IM-PLDPC CODE IN THE GSMPPM SYSTEMS OVER A WEAK TURBULENCE CHANNEL, WHERE $N_t = 4$, $N_r = 4$, $N_t = 2$, AND THE MODULATION PATTERNS ARE (4, 4, 2, 5, 2, 32), (4, 4, 2, 6, 2, 32), (4, 4, 2, 7, 2, 64) AND (4, 4, 2, 8, 2, 64).

Modulation Pattern \ Code Type	(4, 4, 2, 5, 2, 32)	(4, 4, 2, 6, 2, 32)	(4, 4, 2, 7, 2, 64)	(4, 4, 2, 8, 2, 64)
Regular	-3.3336	-3.4893	-3.8719	-4.1558
AR4JA	-3.6942	-3.7542	-4.3475	-4.4732
Code-B	-2.7952	-2.9986	-3.5719	-3.8209
IM-PLDPC	-3.7918	-3.8892	-4.4693	-4.5256

their associated edges. In a protograph, parallel edges are allowed. In addition, the protograph with a code rate $R = (p_c - p_v)/p_c$ can be represented by a base matrix $\mathbf{B}_o = (b_{i,j})$ of size $p_c \times p_v$, where $b_{i,j}$ denotes the number of edges connecting CN c_i and VN v_j . A large protograph (resp. parity-check matrix) of size $P_c \times P_v$ corresponding to the PLDPC code, can be constructed by performing a lifting operation on a given protograph (resp. base matrix), where $P_c = Tp_c$, $P_v = Tp_v$ and T denotes a lifting factor. Typically, the lifting operation (i.e., copy and permute) can be implemented by a modified progressive-edge-growth (PEG) algorithm [37].

It is well known that the BER performance of a PLDPC code may show different performance in different communication scenarios. For specific communication scenarios, it is essential to design PLDPC codes with outstanding performance. In the PLDPC code design, a pre-coding structure and a certain proportion of degree-2 VNs can improve the decoding thresholds [27],

TABLE V
TMDRS OF THE RATE-1/2 AR4JA CODE, REGULAR-(3,6) CODE, CODE-B AND THE PROPOSED IM-PLDPC CODE.

Code Type	IM-PLDPC	AR4JA	Regular	Code-B
TMDR	0.007	0.014	0.023	N.A.

[38]. Nevertheless, as the typical minimum distance ratio (TMDR) [39] is extremely susceptible to degree-2 VNs, a finite-length code with excessive degree-2 VNs always has error floor in the high SNR region. For instance, the accumulate-repeat-3-accumulate (AR3A) code [27] and the AR4JA code possess two degree-2 VNs and one degree-2 VN, respectively. According to the analyses, the AR3A code does not possess TMDR and has an error floor in the high SNR region. Conversely, the AR4JA codes benefits from TMDR and does not have any error floor in the high SNR region [27]. As such, some constraints should be imposed on the protograph at the initial stage of PLDPC-code design, as follows.

- 1) A pre-coding structure: the pre-coding structure includes a CN and two VNs. Especially, the CN connects only a degree-1 VN and a highest-degree punctured VN.
- 2) Appropriate proportion of degree-2 VNs: If the number of CNs is p_c , the number of degree-2 VNs must satisfy $1 \leq p_{v,2} \leq p_c/2$. Otherwise, TMDR cannot be guaranteed.
- 3) Low complexity: To ensure the low encoding/decoding complexity, the number of parallel edges connecting the CN c_i and the VN v_j is limited up to 3 (i.e., $b_{i,j} \in \{0, 1, 2, 3\}$). To further reduce the search space, an additional constraint is imposed, i.e., $b_{1,5} + b_{2,5} + b_{3,5} + b_{4,5} = b_{1,6} + b_{2,6} + b_{3,6} + b_{4,6} = b_{1,7} + b_{2,7} + b_{3,7} + b_{4,7} > 2$.

Taking into account the three constraints discussed above, we design a new PLDPC code with excellent performance in the PLDPC-coded GSMPPM system. Specifically, in order to reduce the computational complexity for search, we consider a rate-1/2 PLDPC code and a 4×7 base matrix containing 28 elements. The corresponding initial base matrix \mathbf{B}_o can be expressed as

$$\mathbf{B}_o = \begin{bmatrix} 1 & 0 & 0 & b_{1,4} & b_{1,5} & b_{1,6} & b_{1,7} \\ 0 & 1 & 1 & b_{2,4} & b_{2,5} & b_{2,6} & b_{2,7} \\ 0 & 0 & 1 & b_{3,4} & b_{3,5} & b_{3,6} & b_{3,7} \\ 0 & 1 & 0 & b_{4,4} & b_{4,5} & b_{4,6} & b_{4,7} \end{bmatrix}. \quad (7)$$

After a simple search with a PEXIT algorithm [33], [36], one can obtain the rate-1/2 improved PLDPC code, referred to as *IM-PLDPC code*, which enables the lowest decoding threshold and

effective TMDR. The base matrix \mathbf{B}_{IM} is represented as

$$\mathbf{B}_{\text{IM}} = \begin{bmatrix} 1 & 0 & 0 & 2 & 0 & 0 & 0 \\ 0 & 1 & 1 & 3 & 1 & 1 & 0 \\ 0 & 0 & 1 & 1 & 2 & 2 & 1 \\ 0 & 1 & 0 & 2 & 0 & 0 & 2 \end{bmatrix}, \quad (8)$$

where the fourth column denotes a punctured VN and the total number of edges is 22.

B. Performance Analysis

Referring to Table IV, we compare the decoding thresholds of the rate-1/2 IM-PLDPC code with those of three other existing codes (i.e., the AR4JA code [27], regular-(3,6) code [40], and the optimized code-B [28]) in the GSMPPM system over a weak turbulence channel. It is revealed that the IM-PLDPC code achieves gains about 0.1 dB, 0.45 dB and 0.99 dB compared to the AR4JA code, regular-(3,6) code and code-B in (4,4,2,5,2,32) GSMPPM, respectively. Similar results can be obtained from the (4,4,2,6,2,32) GSMPPM. Moreover, when the spectral efficiency $\rho = 6$ bpcu (i.e., (4,4,2,7,2,64) and (4,4,2,8,2,64) GSMPPM schemes), the decoding thresholds of the IM-PLDPC code are better than the other counterparts.

Furthermore, we measure the TMDRs of the IM-PLDPC code, AR4JA code, regular-(3,6) code, code-B by utilizing the AWD function [39]. Referring to Table V, we observe that the IM-PLDPC code, AR4JA code and regular-(3,6) code possess effective TMDRs, while code-B does not have a TMDR. It implies that the IM-PLDPC code enjoys the linear-minimum-distance-growth property and does not suffer from an error floor in the high SNR region.

Based on the above analyses, it can be derived that the IM-PLDPC code has desirable error performance in both the low and high SNR regions in the GSMPPM systems.

V. SIMULATION RESULTS

In this section, we provide simulations of the PLDPC-coded GSMPPM systems with the proposed ADM constellations, the optimized constellations and three existing constellations (i.e., natural [35], GSL [4], MCSS [17] constellations) over weak turbulence channels. We also compare the bit-error-rates (BERs) of the proposed IM-PLDPC code, AR4JA code [27], regular-(3,6) code [40], and the optimized code-B [28] in such scenarios. Unless otherwise mentioned, we assume that transmitted codeword length $s = 4500$, and the maximum number of BP iterations t_{BP} is 100.

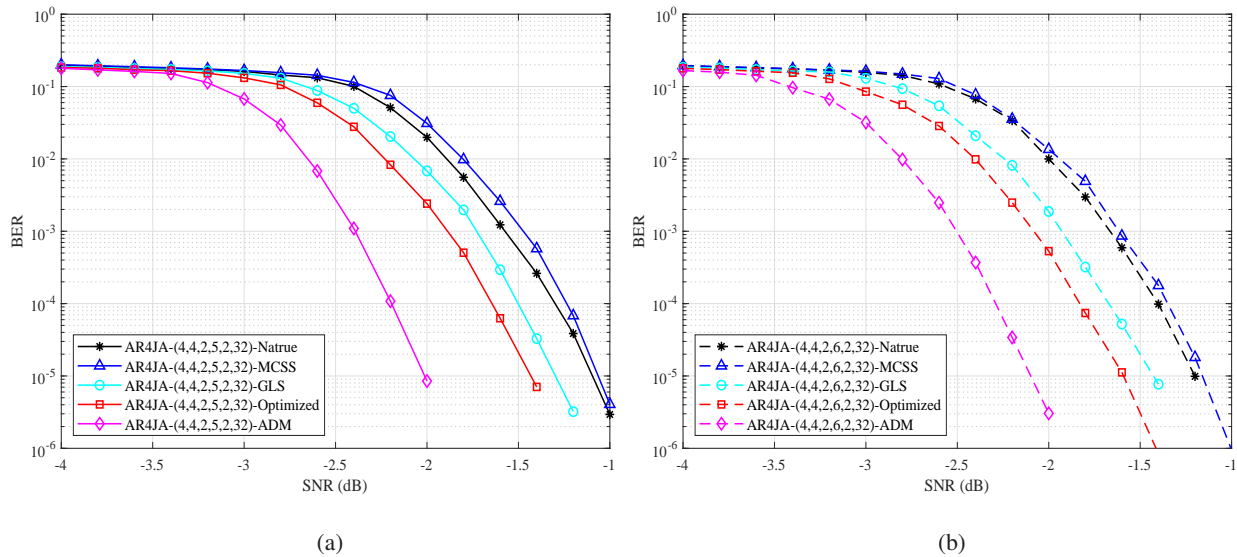


Fig. 4. BER curves of the AR4JA-coded GSMPPM systems with the proposed ADM constellation, the optimized constellation, natural constellation, MCSS constellation, and GLS constellation: (a) $(4, 4, 2, 5, 2, 32)$ GSMPPM with $\rho = 5$ bpcu; (b) $(4, 4, 2, 6, 2, 32)$ GSMPPM with $\rho = 5$ bpcu.

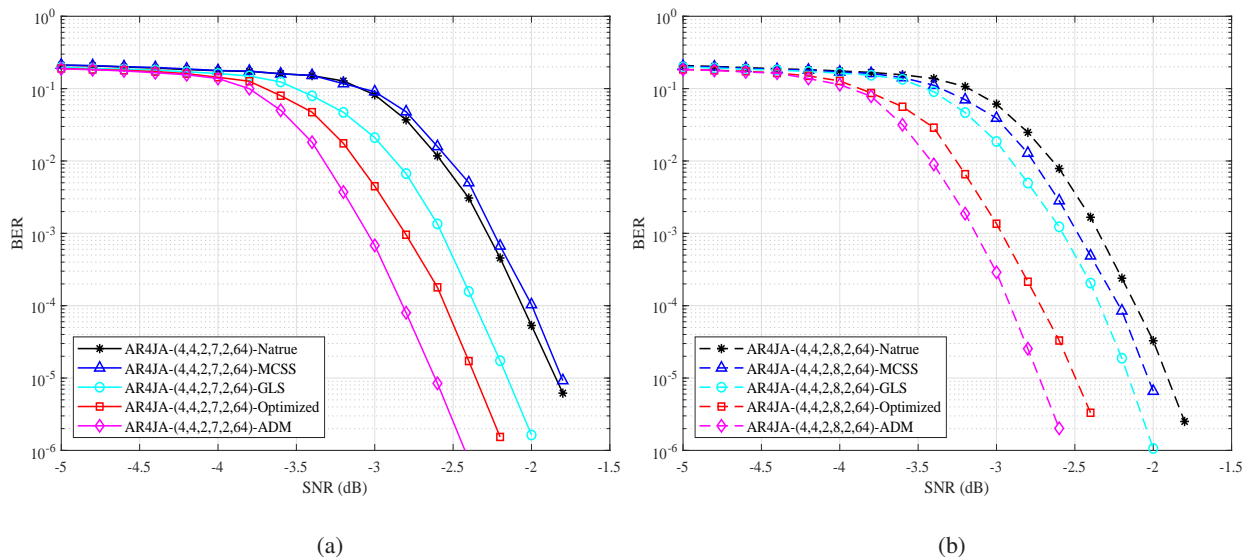


Fig. 5. BER curves of the AR4JA-coded GSMPPM systems with the proposed ADM constellation, the optimized constellation, natural constellation, MCSS constellation, and GLS constellation: (a) $(4, 4, 2, 7, 2, 64)$ GSMPPM with $\rho = 6$ bpcu; (b) $(4, 4, 2, 8, 2, 64)$ GSMPPM with $\rho = 6$ bpcu.

A. BER Performance of Different GSMPPM Constellations

In Fig. 4, we consider the AR4JA-coded GSMPPM systems with the spectral efficiency $\rho = 5$ bpcu. As seen from Fig. 4(a), the AR4JA code with the proposed ADM constellation exhibits better performance compared to the other four constellations in $(4, 4, 2, 5, 2, 32)$ GSMPPM scheme.

Specifically, at a BER of 10^{-5} , the proposed ADM constellation has about 0.4 dB, 0.6 dB, 0.9 dB and 0.8 dB gains over the optimized constellation, GSL constellation, MCSS constellation and natural constellation, respectively. As illustrated in Fig. 4(b), similar performance can be obtained for (4, 4, 2, 6, 2, 32) GSMPPM scheme. When the spectral efficiency $\rho = 6$ bpcu, Fig. 5 shows the BER curves of the AR4JA-coded GSMPPM systems with five different constellations. In Fig. 5(a), the proposed ADM constellation requires -2.62 dB to obtain a BER of 10^{-5} , while the natural, GSL, MCSS and the optimized constellations require -1.85 dB, -1.81 dB, -2.15 dB and -2.36 dB, respectively. Likewise, Fig. 5(b) also shows that the proposed ADM constellation requires the smallest SNR to achieve a BER of 10^{-5} in (4, 4, 2, 8, 2, 64) GSMPPM scheme.

In addition, simulation results are consistent with the decoding-threshold analysis in Section III-B (see Table III). Therefore, we can conclude that the proposed ADM constellations are well suited to the PLDPC-coded GSMPPM systems.

B. BER Performance of Different PLDPC Codes

Fig. 6 shows the BER curves of the proposed IM-PLDPC code, regular-(3, 6) code [40], AR4JA code [27], and the optimized code-B [28] in the GSMPPM systems with the spectral efficiency $\rho = 5$ bpcu. In Fig. 6(a), we can see that at a BER of 10^{-5} , the IM-PLDPC code respectively obtains about 0.4 dB, 0.5 dB and 0.8 dB gain compared to the AR4JA code, the regular-(3, 6) code and the code-B in (4, 4, 2, 5, 2, 32) GSMPPM scheme. Similar BER simulation results can also be observed in the case of (4, 4, 2, 6, 2, 32) GSMPPM (see Fig. 6(b)). On the other hand, when the spectral efficiency $\rho = 6$ bpcu, Fig. 7 show that IM-PLDPC code does not exhibit any error floor in the high SNR region. Specifically, Fig. 7(a) shows that the IM-PLDPC code needs about -2.95 dB to obtain a BER of 10^{-5} in (4, 4, 2, 7, 2, 64) GSMPPM, while the regular-(3, 6) code, the AR4JA code and code-B require -2.52 dB, -2.62 dB and -2.15 dB, respectively, to do so. In (4, 4, 2, 8, 2, 64) GSMPPM scheme, the IM-PLDPC code also exhibits the lowest SNR to achieve a BER of 10^{-5} , as shown in Fig. 7(b). Based on the above discussion, the IM-PLDPC code is promising to be used in the PLDPC-coded GSMPPM systems.

Remark: We have also carried out analyses and simulations with other parameter settings (i.e., different values of N_t , N_r , N_a , l , l_a , and σ_x) and obtained similar observations, which substantially demonstrate the superiority of our proposed constellations and code design.

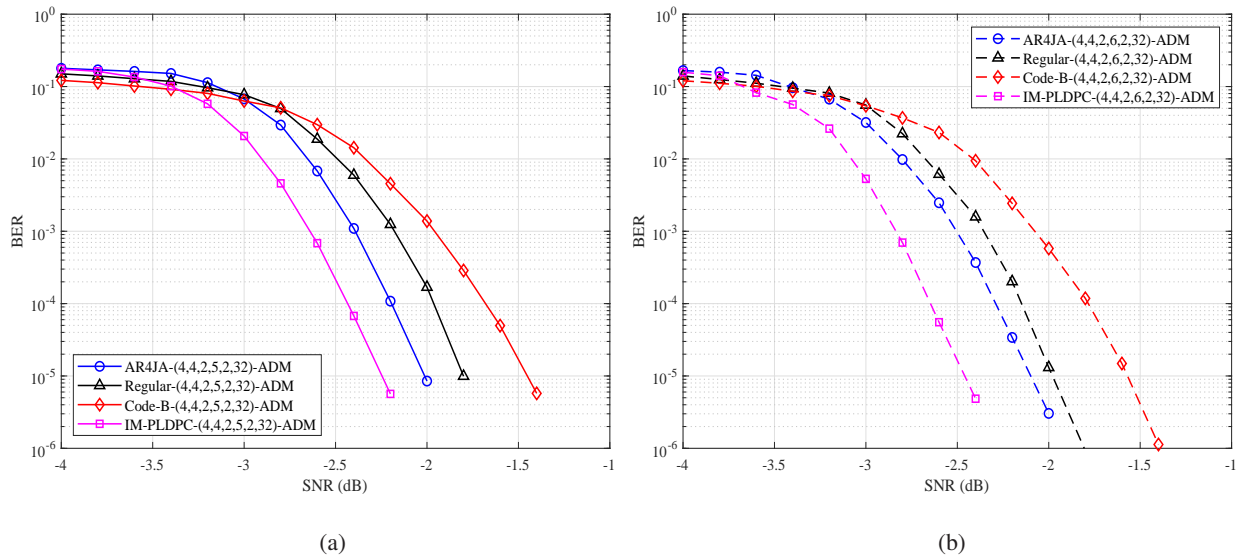


Fig. 6. BER curves of the IM-PLDPC code, AR4JA code, regular-(3, 6) code and code-B with the proposed ADM constellations in GSMPPM systems: (a) (4, 4, 2, 5, 2, 32) GSMPPM with $\rho = 5$ bpcu; (b) (4, 4, 2, 6, 2, 32) GSMPPM with $\rho = 5$ bpcu.

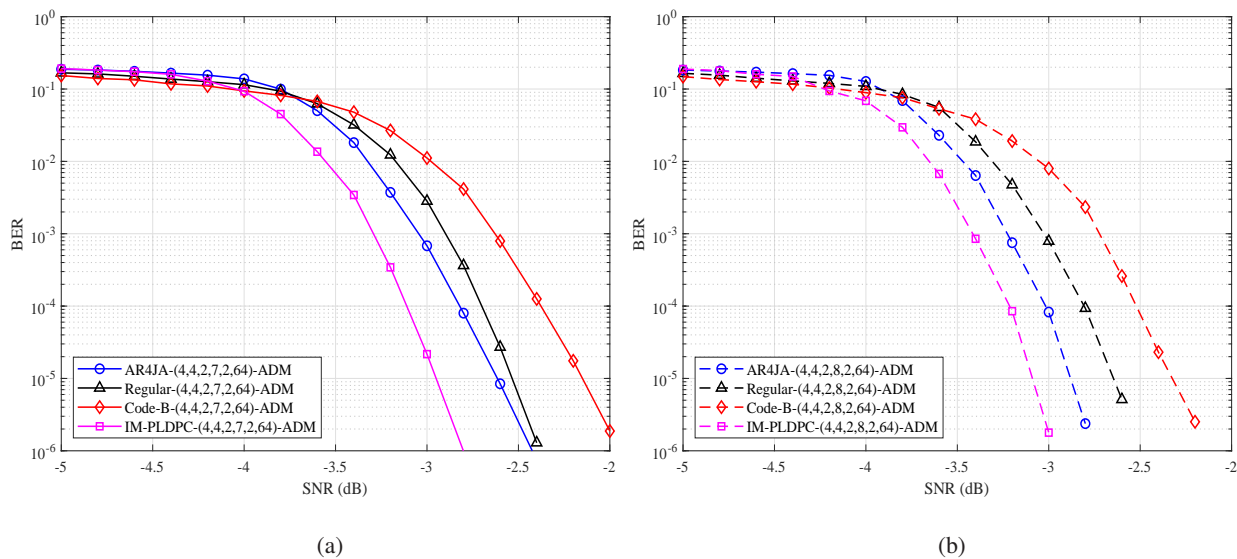


Fig. 7. BER curves of the IM-PLDPC, AR4JA code, regular-(3, 6) code and code-B with the proposed ADM constellations in GSMPPM systems: (a) (4, 4, 2, 7, 2, 64) GSMPPM with $\rho = 6$ bpcu; (b) (4, 4, 2, 8, 2, 64) GSMPPM with $\rho = 6$ bpcu.

VI. CONCLUSION

This paper investigated the performance of PLDPC-coded GSMPPM systems over weak turbulence channels. We proposed a type of novel GSMPPM constellations, called ADM constellations, which can achieve desirable capacities and convergence performance in this scenario. Furthermore, we constructed an improved PLDPC code using the PEXIT-aided computer search

method, which possesses desirable decoding threshold and effective TMDR. Theoretical analyses and simulated results indicated that the PLDPC-coded GSMPPM system using the proposed ADM constellations and IM-PLDPC code can exhibit noticeable performance gains with respect to the state-of-the-art counterparts. Based on the appealing advantages, the proposed PLDPC-coded GSMPPM transmission scheme stands out as a competitive alternative for high-reliability FSO applications.

REFERENCES

- [1] A. Elzanaty and M. S. Alouini, "Adaptive coded modulation for IM/DD free-space optical backhauling: a probabilistic shaping approach," *IEEE Trans. Commun.*, vol. 68, no. 10, pp. 6388–6402, Oct. 2020.
- [2] S. R, S. Sharma, N. Vishwakarma, and A. S. Madhukumar, "HAPS-based relaying for integrated space-air-ground networks with hybrid FSO/RF communication: a performance analysis," *IEEE Trans. Aerosp. Electron. Syst.*, vol. 57, no. 3, pp. 1581–1599, Jun. 2021.
- [3] H. Nouri and M. Uysal, "Adaptive MIMO FSO communication systems with spatial mode switching," *J. Opt. Commun. Netw.*, vol. 10, no. 8, pp. 686–694, Aug. 2018.
- [4] T. T. Nguyen and L. Lampe, "Coded multipulse pulse-position modulation for free-space optical communications," *IEEE Trans. Commun.*, vol. 58, no. 4, pp. 1036–1041, Apr. 2010.
- [5] T. V. Pham, T. C. Thang, and A. T. Pham, "Average achievable rate of spatial diversity MIMO-FSO over correlated gamma-gamma fading channels," *J. Opt. Commun. Netw.*, vol. 10, no. 8, pp. 662–674, Aug. 2018.
- [6] M. A. Khalighi and M. Uysal, "Survey on free space optical communication: a communication theory perspective," *IEEE Commun. Surveys Tuts.*, vol. 16, no. 4, pp. 2231–2258, 4th Quarter 2014.
- [7] S. Sharma, A. Madhukumar, and S. R, "MIMO hybrid FSO/RF system over generalized fading channels," *IEEE Trans. Veh. Technol.*, vol. 70, no. 11, pp. 11 565–11 581, Nov. 2021.
- [8] A. A. Youssef, M. Abaza, and A. S. Alatawi, "LDPC decoding techniques for free-space optical communications," *IEEE Access*, vol. 9, pp. 133 510–133 519, Sept. 2021.
- [9] M. Elamassie and M. Uysal, "Incremental diversity order for characterization of FSO communication systems over lognormal fading channels," *IEEE Commun. Lett.*, vol. 24, no. 4, pp. 825–829, Apr. 2020.
- [10] X. Zhu and J. M. Kahn, "Performance bounds for coded free-space optical communications through atmospheric turbulence channels," *IEEE Trans. Commun.*, vol. 51, no. 8, pp. 1233–1239, Aug. 2003.
- [11] R. Yuan and J. Cheng, "Free-space optical quantum communications in turbulent channels with receiver diversity," *IEEE Trans. Commun.*, vol. 68, no. 9, pp. 5706–5717, Sept. 2020.
- [12] K. J. Jung, S. S. Nam, J. Shin, and Y. C. Ko, "Unified statistical performance of FSO link due to the combined effect of weak turbulence and generalized pointing error with HD and IM/DD," *J. Commun. Netw.*, vol. 22, no. 6, pp. 476–483, Dec. 2020.
- [13] A. E. Morra, H. S. Khallaf, H. M. H. Shalaby, and Z. Kawasaki, "Performance analysis of both shot- and thermal-noise limited multipulse PPM receivers in gamma-gamma atmospheric channels," *J. Light. Technol.*, vol. 31, no. 19, pp. 3142–3150, Oct. 2013.
- [14] Z. Li, H. Yu, B. Shan, D. Zou, and S. Li, "New run-length limited codes in on-off keying visible light communication systems," *IEEE Wireless Commun. Lett.*, vol. 9, no. 2, pp. 148–151, Feb. 2020.

- [15] F. Xu, M. Khalighi, and S. Bourennane, "Coded PPM and multipulse PPM and iterative detection for free-space optical links," *J. Opt. Commun. Netw.*, vol. 1, no. 5, pp. 404–415, Oct. 2009.
- [16] H. Sugiyama and K. Nosu, "MPPM: a method for improving the band-utilization efficiency in optical PPM," *J. Light. Technol.*, vol. 7, no. 3, pp. 465–472, Mar. 1989.
- [17] S. Lou, C. Gong, N. Wu, and Z. Xu, "Joint dimming and communication design for visible light communication," *IEEE Commun. Lett.*, vol. 21, no. 5, pp. 1043–1046, May 2017.
- [18] M. Miao and X. Li, "Novel approximate distribution of the sum of lognormal-rician turbulence channels with pointing errors and applications in MIMO FSO links," *IEEE Photon. J.*, vol. 14, no. 4, pp. 1–15, Aug. 2022.
- [19] W. O. Popoola, E. Poves, and H. Haas, "Spatial pulse position modulation for optical communications," *J. Light. Technol.*, vol. 30, no. 18, pp. 2948–2954, Sept. 2012.
- [20] H. G. Olanrewaju, J. Thompson, and W. O. Popoola, "Generalized spatial pulse position modulation for optical wireless communications," in *Proc. IEEE 84th Veh. Technol. Conf. (VTC-Fall)*, Sept. 2016, pp. 1–5.
- [21] T. C. Bui, M. Biagi, and S. Kiravittaya, "Theoretical analysis of optical spatial multiple pulse position modulation," in *Proc. IEEE Global Commun. Conf. (GLOBECOM)*, Dec. 2018, pp. 1–7.
- [22] T. K. Nguyen, C. T. Nguyen, H. D. Le, and A. T. Pham, "TCP performance over satellite-based hybrid FSO/RF vehicular networks: modeling and analysis," *IEEE Access*, vol. 9, pp. 108 426–108 440, Aug. 2021.
- [23] Sonali, A. Dixit, and V. K. Jain, "Analytical determination of thresholds of LDPC codes in free space optical channel," *IEEE Open J. Commun. Soc.*, vol. 2, pp. 35–47, Nov. 2021.
- [24] H. Jiang, N. He, X. Liao, W. Popoola, and S. Rajbhandari, "The BER performance of the LDPC-coded MPPM over turbulence UWOC channels," *Photonics*, vol. 9, no. 5, p. 349, May 2022.
- [25] J. Thorpe, "Low-density parity-check (LDPC) codes constructed from protographs," *IPN Progr. Rep.*, vol. 42, no. 154, pp. 42–154, Aug. 2003.
- [26] S. Y. Chung, G. D. Forney, T. J. Richardson, and R. Urbanke, "On the design of low-density parity-check codes within 0.0045 dB of the shannon limit," *IEEE Commun. Lett.*, vol. 5, no. 2, pp. 58–60, Feb. 2001.
- [27] Y. Fang, G. Bi, Y. L. Guan, and F. C. M. Lau, "A survey on protograph LDPC codes and their applications," *IEEE Commun. Surveys & Tutorials*, vol. 17, no. 4, pp. 1989–2016, 4th Quarter 2015.
- [28] H. Zhou, M. Jiang, C. Zhao, and J. Wang, "Optimization of protograph-based LDPC coded BICM-ID for the poisson PPM channel," *IEEE Commun. Lett.*, vol. 17, no. 12, pp. 2344–2347, Dec. 2013.
- [29] M. V. Jamali, A. Mirani, A. Parsay, B. Abolhassani, P. Nabavi, A. Chizari, P. Khorramshahi, S. Abdollahramezani, and J. A. Salehi, "Statistical studies of fading in underwater wireless optical channels in the presence of air bubble, temperature, and salinity random variations," *IEEE Trans. Commun.*, vol. 66, no. 10, pp. 4706–4723, Oct. 2018.
- [30] C. Li, Y. Cheng, Y. Zhang, and Y. Huang, "Low-complexity soft-output detectors for LDPC coded spatial modulation systems," in *Proc. Int. Conf. Wireless Commun. Signal Process., Nanjing, China*, Oct. 2015, pp. 1–6.
- [31] F. R. Kschischang and B. J. Frey, "Iterative decoding of compound codes by probability propagation in graphical models," *IEEE J. Sel. Areas Commun.*, vol. 16, no. 2, pp. 219–230, Feb. 1998.
- [32] Y. Fang, P. Chen, G. Cai, F. C. M. Lau, S. C. Liew, and G. Han, "Outage-limit-approaching channel coding for future wireless communications: root-protograph low-density parity-check codes," *IEEE Veh. Technol. Mag.*, vol. 14, no. 2, pp. 85–93, Jun. 2019.
- [33] Z. Yang, Y. Fang, Y. Cheng, P. Chen, and D. Almakhlles, "Protograph LDPC-coded BICM-ID with irregular mapping: an emerging transmission technique for massive internet of things," *IEEE Trans. Green Commun. Netw.*, vol. 5, no. 3, pp. 1051–1065, Sept. 2021.

- [34] Z. Wu, X. Gao, and C. Jiang, "Nonbinary LDPC-coded spatial multiplexing for rate-2 MIMO of DVB-NGH system," *IEEE Trans. Broadcast.*, vol. 64, no. 2, pp. 201–210, Jun. 2018.
- [35] S. Liu, "Improved coding techniques for MPPM-like systems," Ph.D. dissertation, University of Toronto, Toronto, Canada, 2009.
- [36] L. Dai, Y. Fang, Z. Yang, P. Chen, and Y. Li, "Protograph LDPC-coded BICM-ID with irregular CSK mapping in visible light communication systems," *IEEE Trans. Veh. Technol.*, vol. 70, no. 10, pp. 11 033–11 038, Oct. 2021.
- [37] V. Nguyen, "Design of capacity-approaching protograph-based LDPC coding systems," Ph.D. dissertation, Dept. Electr. Eng. Univ. Texas at Dallas, Dallas, TX, USA, Dec. 2012.
- [38] T. V. Nguyen, A. Nosratinia, and D. Divsalar, "The design of rate-compatible protograph LDPC codes," *IEEE Trans. Commun.*, vol. 60, no. 10, pp. 2841–2850, Oct. 2012.
- [39] D. Divsalar, S. Dolinar, C. R. Jones, and K. Andrews, "Capacity-approaching protograph codes," *IEEE J. Sel. Areas Commun.*, vol. 27, no. 6, pp. 876–888, Aug. 2009.
- [40] Y. Tan, J. Guo, Y. Ai, W. Liu, and Y. J. Fei, "A coded modulation scheme for deep-space optical communications," *IEEE Photon. Technol. Lett.*, vol. 20, no. 5, pp. 372–374, Mar. 2008.